

## A Numerical Model For Performance Prediction of Dry Cooling Conditions of Air Cooled Condensers In Thermal Power Plant Stations

Dr. Ali Hussain Tarrad\*

Received on:17/1/2010

Accepted on:6/5/2010

### Abstract:

The present work represents theoretical treatment of dry cooling of the air cooled condensers applied in the power plants technology. A suggested model was built in a form of computer program to predict the effectiveness of the condenser showing the effect of inlet air temperature and its mass flow rate on the performance of the condenser. The model construction depends on the idea of using a *row by row* marching solution for energy balance for both stream sides. The model has the ability to estimate the heat transfer coefficient, air temperature and other air physical properties distribution in the air flow direction from row to row. The results showed that using the cooling process of the air before entering the condenser improves the performance of the condenser and reduces the required area for a specified condensation load and steam loading. For fixed surface area of the condenser, lowering the dry bulb temperature from (45) to (28)°C at a constant wet bulb temperature and mass flow rate of the entering air can improve the condensation load up to (23 %) for the present investigated conditions.

**Keywords:** Condensers, Performance, Steam, Power Plants, Dry Cooling, Phase Change, Design

### نموذج عددي للتنبؤ بأداء المكثفات المبردة بالهواء تحت ظروف التبريد الجاف في محطات الطاقة الحرارية

#### الخلاصة

يتضمن البحث الحالي دراسة نظرية للمكثفات المزعفة والمبردة بالهواء تحت ظروف التبريد الجاف والمستخدمة في محطات الطاقة الحرارية. النموذج المقترح تم بناؤه لغرض التنبؤ بالفعالية للمكثف مبيناً تأثير درجة حرارة البصلة الجافة ومعدل تدفق الهواء الداخل للمبادل على أداء المكثف. النموذج يعتمد على فكرة تطبيق الاتزان الحراري لكل صف من الأنابيب باتجاه جريان الهواء ولكلا الجانبين للمكثف. النموذج المقترح له الإمكانية لتخمين توزيع معامل انتقال الحرارة، درجة حرارة الهواء وجميع المواصفات الفيزيائية الأخرى باتجاه جريان الهواء من صف لآخر. قد بينت النتائج إن استخدام التبريد للهواء قبل دخوله للمكثف يمكن أن يحسن كثيراً من أداء المبادل ويقلل من المساحة السطحية للمكثف لقيم محددة من حمل التكثيف ومعدل جريان ثابت من بخار الماء. لمساحة سطحية ثابتة للمكثف فإن تخفيض درجة حرارة البصلة الجافة للهواء الداخل للمكثف من (45) إلى (28) م° بثبوت درجة حرارة البصلة الرطبة ومعدل الجريان الكتلي يمكن أن يزيد حمل التكثيف بمقدار (23 %) للظروف التشغيلية التي تم اختبارها خلال ألبحث الحالي.

**Introduction:**

Due to the excessive demand for water for both domestic and industrial use for water cooled condensers in the thermal power plant technology and the continuously decrease in the water resources, the dry cooling is one of the best remedies to this problem. Dry cooling of power plants may be considered as an attractive alternative to wet cooling particularly where water conservation and environmental protection pose critical sitting issue. However, the dry cooling may not be able to maintain design plant output during the hottest periods of the year.

**Larinoff** and **Moles** (1978) [1] outlined the problems that may be arise in the operation of the air cooled steam condensers. They investigated the effect of the ambient temperature on the turbine backpressure. **Ganapathy** (1982) [2] concluded that for air- cooled condensers ambient air is the most important variable in the design. Since ambient temperature in a location varies throughout the year, a higher value, if used, would result in over sizing the unit. A lower value would give poor performance. **Berger** (2000) [3] showed that the air cooled condenser of the A-frame, **figure (1)**, design not only does facilitate condensate draining and collection but also ensures that there are no dead zones in the heat transfer surface, that there is a high operating stability during load transient. **Kröger** (1998) [4] stated that the major performance and cost issue with dry cooling has

been the limitation on performance during the hottest days of the year, where the use of dry cooling can limit plant output and decrease plant efficiency. Therefore, *the investigated enhancement schemes have focused on the use of a limited amount of water during the hottest hours.*

**Micheletti** and **Burns** (1992) [5] found that for dry cooling systems, sensible heat transfer is the only form of heat rejection, therefore the performance depends upon the ambient air dry-bulb temperature instead of the wet bulb temperature. The **U.S. Environmental Protection Agency** (2000) [6] conducted a comparative study of the environmental impacts of wet vs. dry cooling. They concluded that the energy consumption per (lb) condensate was higher for dry cooling than for wet cooling and that the atmospheric emission associated with energy consumption was also higher. **Maulbetsch** and **DiFilippo** (2003) [7] investigated the use of low pressure spray enhancement system to address the efficiency and capacity penalties of dry cooling. They concluded that a few degrees reduction in the inlet air temperature can restore much of the lost plant capacity during hot hours. *However, it increases the potential for the scaling and corrosion of the air cooled heat exchangers.*

**Tarrad** and **Shehhab** (2007) [8] have presented a procedure for the thermal and hydrodynamics design of the plate finned tube heat exchanger. The dehumidification of air as it passes across the heat exchanger was taken into account. **Tarrad et al.** (2009)[9] presented a two

dimensional model to perform the core dimensions prediction of the air cooled heat exchanger. The suggested simulation model showed that the overall heat transfer coefficient of the heat exchanger did not change much with the vertical position with respect to the row number and it is essentially a constant value.

In the present work a numerical model based on the row by row marching solution is suggested to predict the *dry cooling* effect of entering air temperature on the condenser loading capacity and thermal load. This mode of condensation enhancement for steam condenser is applied here, since it represents a clean cooling mode avoiding the scaling problem arising from the *wet cooling* mode especially in Iraq severe dusty weather in summer.

**Theoretical Model:**

The present work was incorporated in a numerical analysis for the performance prediction of the *air cooled steam condenser*. The model is based on the idea of a marching solution for the heat exchanger in the air flow direction. **Figure (2)** shows a schematic diagram of the tube arrangement of air cooled heat exchanger having three tube rows. It is suggested to solve the energy balance equation between the steam condensation side and the cooling air side for each tube row. A step by step technique is applied for the heat exchanger assuming that the exit air condition from a row of tubes of the heat exchanger as the entering condition to the next tube row and so on until the

exit side of the heat exchanger. In this procedure a variable air properties may be incorporated in the solution scheme and reducing the effect of property variation on the air side heat transfer coefficient.

**Tube Side Heat Transfer Coefficient:**

The heat transfer coefficient of the tube side for the complete condensation of steam can be estimated from the available empirical correlations in the open literature. The *Nusselt* model (1916) [10] gives the heat transfer coefficient for the laminar condensation ( $Re_l \leq 30$ ) inside vertical tubes in the form:

$$h_c = 0.943 \left\{ \frac{\rho_l(\rho_l - \rho_v)g h_{fg} k_l^3}{L \mu_l (T_v - T_w)} \right\}^{1/4} \dots(1)$$

*McAdams* (1954) [11] suggested to adopt a (20%) increase to the estimated value by the above equation to compensate the ripple effect that introduced by the condensate film. Here, he has altered the coefficient (0.943) to a value of (1.13) in the above correlations. To include the effect of tube inclination arrangement on the heat transfer coefficient *Dhir* and *Lienhard* (1971) [12] suggested to replace the gravitational force with its component parallel to heat transfer area. Therefore, eq. (1) would have the form:

$$h_c = 1.13 \left\{ \frac{\rho_l(\rho_l - \rho_v)g h_{fg} k_l^3 \sin \theta}{L \mu_l (T_v - T_w)} \right\}^{1/4} \quad (2.a)$$

In which the latent heat of vaporization is corrected in the form postulated by *Rohsenow* (1956) [13] as:

$$h_{fg} = h_{fg} + 0.68cp_l (T_v - T_w) \dots(2.b)$$

In the laminar wavy region, ( $30 \leq Re_l \leq 1800$ ), *Kutateladze* (1963) [14] recommended the following correlation:

$$h_c = \frac{k_l}{(v_l^2/g)^{1/5}} \frac{Re_l}{1.088 Re_l^{1.25} - 5.2} \dots (3)$$

The gravitational force with its component parallel to heat transfer area should be used for the inclined surface application suggested in the present work.

For the turbulent condensation ( $Re_l \geq 1800$ ) conditions inside tubes *Kirkbride* (1934) [15] developed an empirical simple formula in the form:

$$h_c = 0.0077 x Re_l^{0.4} \dots\dots\dots (4.a)$$

Where  $x = \left\{ \frac{\rho_l (\rho_l - \rho_v) g h_i^3}{\mu_l^2} \right\}^{1/3} \dots\dots\dots (4.b)$

$$Re_l = \frac{4 \Gamma_v}{\mu_l} \dots\dots\dots (4.c)$$

$$\Gamma_v = \frac{\dot{m}_c}{N_t \pi d_i} \dots\dots\dots (4.d)$$

In the present work it is suggested to use the gravitational force component parallel to the surface in the above equation for the inclination effect of the heat exchanger as follows:

$$h_c = 0.0077 x Re_l^{0.4} \dots\dots\dots (5.a)$$

Where  $x = \left\{ \frac{\rho_l (\rho_l - \rho_v) g h_i^3 \sin \theta}{\mu_l^2} \right\}^{1/3} \dots (5.b)$

*Labuntsov* (1957) [16] recommended the following correlation for the turbulent condensation where Reynolds number ( $Re_l \geq 1800$ ) in the form:

$$h_c = \left( \frac{h_l}{(v_l^2/g)^{1/3}} \right) y' \dots\dots\dots (6.a)$$

$$y' = \frac{Re_l}{8720 + 18.8 Re_l^{0.8} (Re_l^{0.75} - 225)} \dots\dots (6.b)$$

The gravitational force parallel to the surface will be used in this correlation to yield:

$$h_c = \left( \frac{h_l}{(v_l^2/g \sin \theta)^{1/3}} \right) y' \dots\dots\dots (6.c)$$

It is important to mention here that all of the above correlations for the condensation heat transfer coefficient represent a mean value for whole of the tube surface. The above correlations showed acceptable agreement with the

experimental data of steam condensation.

**Air Side Heat Transfer Coefficient:**

The air side heat transfer coefficient for the continuous plate fin of the present work can be estimated by the well known method developed by *McQuiston* (1988) [17]. He has adopted the scheme presented by *Schmidt* (1946) [18] and extended it for the continuous hexagonal plate fins, **figure (3)**. A detailed procedure for the circular tube section has been outlined by *Tarrad* and *Shehhab* [8]. The elliptic cross section tube was also considered in detailed procedure by *Tarrad et al.* (2008) [19] and *Tarrad et al.* [9]. The latter scheme will be used in the present work for the estimation of the air side heat transfer coefficient.

The following points should be considered for this procedure:

- i- For the case in this study where the tube bundle is in the vertical orientation, inline tube arrangement, and elliptical tube shape, the minimum flow area may be expressed as:

$$A_{min} = H \times (1 - f_{pm} \times t) \times (W - (N_t \times x_c)) \dots (7)$$

- ii- For elliptic tube shape, it is suggested in the present work to replace the inside tube diameter with equivalent diameter calculated on the basis of the same cross sectional area that can handle

the same mass flow rate and fluid velocity.

iii- In the present work, it is suggested that the *Reynold's* number of the air side in the *McQuiston* model to be based on the equivalent tube diameter wherever it is required calculated from:

$$D_e = \frac{4A_e}{p} \dots\dots\dots (8)$$

Where (p) is the wetted perimeter of the tube geometry.

iv- The convective heat transfer coefficient of the air side was given by:

$$h_o = \frac{j \times cp_a \times G_{max}}{(Pr_a)^{2/3}} \dots\dots\dots (9.a)$$

Where the mass velocity through minimum flow area ( $G_{max}$ ) is presented in:

$$G_{max} = \frac{\dot{m}_a}{A_{min}} \dots\dots\dots (9.b)$$

*McQuiston* found that the j-factor for a four row finned tube heat exchanger fits a linear model based on the parameter (JP).

$$j_4 = 0.2675 \times JP + 1.325 \times 10^{-6} \dots\dots\dots (9.c)$$

$$\text{and } JP = Re_D^{-0.4} \times \left( \frac{A_o}{A_t} \right)^{-0.15} \dots\dots\dots (9.d)$$

Here ( $A_t$ ) represents the area of the bare tubes without fins and ( $A_o$ ) is the total air side heat transfer area, fins and tubes. The heat transfer coefficient for heat exchangers with

four or less rows can be found using the following correlation:

$$\frac{j_n}{j_4} = \frac{1 - (1280)(n)(Re_L)_a^{-1.2}}{1 - (1280)(4)(Re_L)_a^{-1.2}} \dots\dots\dots (9.e)$$

The maximum mass velocity, at minimum flow area of the tube bank should be used with the above equations.

To find out the overall surface efficiency for finned tube heat exchanger, it is necessary to determine the efficiency of the fins alone. The total air side surface efficiency is given by:

$$h_{so} = 1 - \frac{A_f}{A_o} \times (1 - h_f) \dots\dots\dots (10.a)$$

In this formula, ( $A_f$ ) represents the total fin surface area. The fin efficiency ( $h_f$ ) for a circular fin is a function of ( $m$ ,  $r_e$  and  $f'$ ).

$$h_f = \frac{\tanh(m \times r_e \times f')}{(m \times r_e \times f')} \dots\dots\dots (10.b)$$

The empirical relations for the equivalent radius of a hexagonal fin, **figure (3.a)**, and rectangular fin, **figure (3.b)**, were given by *McQuiston*. The equivalent radius of a rectangular fin is presented as:

$$\frac{r_e}{r} = 1.28 \times y \times (b - 0.2)^{1/2} \dots\dots\dots (10.c)$$

The coefficients ( $y$ ) and ( $b$ ) are defined as:

$$y = \frac{M}{r} = \frac{X_T}{2 \times r} \dots\dots\dots (10.d)$$

$$b = \frac{L}{M} = \frac{X_L}{X_T} \dots\dots\dots (10.e)$$

For the fins in this study, the length of the fin is much greater than the thickness, so a parameter ( $m$ ) can be expressed as:

$$m = \left( \frac{2 \times h_o}{k_f \times t} \right)^{1/2} \dots\dots\dots (10.f)$$

For circular tubes, a parameter ( $f'$ ) is defined as:

$$f' = \left[ \frac{r_c}{r} - 1 \right] \left[ 1 + 0.35 \times \ln \left( \frac{r_c}{r} \right) \right] \dots (10.g)$$

**Overall Heat Transfer Coefficient:**

The first step in the thermal design of the heat exchanger is to calculate the overall heat transfer coefficient ( $U_o$ ) which will be based on the air-side area. The overall heat transfer coefficient, ( $U_o$ ) takes into consideration total thermal resistance to heat transfer between both fluids and neglecting the conduction and air side fouling resistances is presented by.

$$\frac{1}{U_o} = \frac{1}{h_o h_{so}} + \frac{1}{h_c (A_i/A_o)} + \frac{1}{h_f (A_i/A_o)} \dots (11)$$

The last term of the above expression represents the effect of the fouling resistance of the steam condensation flowing through the heat exchanger tube bundle. Its magnitude may be obtained experimentally or from tabulated data in the literature for the specified process fluid. In this work a value of (4000)  $W/m^2 K$  for the fouling effect,  $h_f$ , on the steam side was assumed, *Sinnott* (1983) [20].

**Air and Steam Thermal Properties:**

The tabulated property values of both saturated steam and air are obtained from *Incropera* and *De Witt* (1990) [21]. The saturated liquid,  $k$ ,  $\rho$ ,  $cp$ , and  $\mu$ , were correlated as a function of temperature in a least squares polynomial expression. The steam specific volume expression was shown to be more accurate if it was correlated in the form  $v_g = C T^m$  where ( $C$ ) and ( $m$ ) are the constants of the fit. The steam saturated temperature was also correlated in the least squares polynomial form as a function of the absolute working pressure of steam. The air thermal properties,  $k$  and  $\mu$  were correlated in the least squares forms as a function of the dry bulb temperature. The related properties for the humid air condition such as  $T_{aw}$ ,  $W_a$ ,  $h_a$ ,  $v_a$ , and  $\phi$ , were all obtained from correlations presented by *Tarrad* and *Shehhab* [8].

**Marching the Model Solution:**

The suggested iterative numerical scheme in the present work for the prediction of the air cooled steam condenser design is as summarized in the flowchart shown in **figure (4)**. The model is applied only for a vertical or an inclined single tube pass condenser receiving a saturated steam. A number of heat exchangers may be designed for a variety of exit air temperature and optimum design can then be selected. This suggested technique will be applied in the present work with a firm computerized design procedure as described below.

- i. Selecting the tube shape, layout, size, and fin specifications with assumed steam velocity will determine the tube bundle ( $N_t$ ) and heat exchanger physical dimensions

concerning the width and depth for a specified number of rows ( $n$ ) from the following geometrical equations:

$$N_t = \frac{\dot{m}_s}{u_s A_c \rho_s} \dots \dots \dots (12.a)$$

$$Z = (n - 1)X_t + y_t + Z_{clearance} \dots (12.b)$$

And

$$N_r = \frac{N_t}{n} \dots \dots \dots (12.c)$$

$$W = (N_r - 1)X_r + x_t + W_{clearance} \dots (12.d)$$

The air side finned surface area might also be determined per unit length of the tube bundle. Noting that ( $D_o$ ) should be replaced for the circular shape tube instead of ( $y_t$ ) and ( $x_t$ ) used for elliptic tube shape. Here, ( $y_t$ ) and ( $x_t$ ) represent the longest and shortest lengths of the elliptical cross section of the tube geometry respectively.

ii. The energy balance between the steam and cooling air sides should be considered for the design requirements. This was done by specifying the required exit air temperature from the condenser ( $T_{ao}$ ) leads to the mass flow rate estimation for air, that is:

$$\dot{m}_a = \frac{\dot{m}_s h_{fg}}{c_p a (T_{ao,ass} - T_{ai})} \dots \dots \dots (13)$$

In which the humid heat is used instead of the dry air specific heat as (1.02) kJ/kg. K.

iii. For the solution technique considered in the present work, the satisfaction of the energy equation should be verified for each row. Therefore, a row by row solution for both sides is established and the output condition for the air side from a row will be the entering condition for the next row and so on to the last row of the heat exchanger. The tube length which represents the height of the heat exchanger is obtained from assumed values of the row exit air temperature ( $T_{ae, ass.}$ ) and

overall heat transfer coefficient ( $U_{o, ass.}$ ) with the condenser heat load from:

$$A_{o,est} = \frac{\dot{m}_s h_{fg}}{U_{o,ass} \Delta T_m} \dots \dots (14.a)$$

$$\Delta T_m = \frac{\Delta T_i - \Delta T_o}{\ln \frac{\Delta T_i}{\Delta T_o}} \dots \dots \dots (14.b)$$

$$H = \frac{A_{o,est}}{(A_f)_{single} f_{pm} + (1 - f_{pm}) \pi D_o N_r} \dots (14.c)$$

$$(A_f)_{single} = 2(WZ) - (N_r n A_t) + 2(Wt) \dots \dots (14.d)$$

Here ( $A_f$ )<sub>single</sub> refers to the heat transfer area of a single continuous plate fin. The assumed values should be verified before terminating the calculation of any specified row.

iv. Select one of the correlation, eq. (2), eq. (3), eq. (5) or eq. (6.b), presented above for the prediction of the steam condensation heat transfer coefficient depending on the existing condensation mode in the tube. All of those formulae require the condensate properties to be estimated at the film temperature. This will require the assumption of the third variable,  $T_{ws}$ , of the tube surface which should be verified from the energy balance before continuing the solution procedure. Here, the calculated ( $h_c$ ) from the correlation must be checked from the wall temperature estimated by:

$$T_{w,cat} = T_s - \frac{\dot{Q}_{tubes}}{h_c A_t} \dots \dots \dots (15)$$

Where ( $\dot{Q}_{tubes}$ ) is the heat load of a single heat exchanger tube. Then this value is compared with the assumed value until the convergence is established.

v- Estimate the air side heat transfer coefficient, eq. (9), fin efficiency and surface total efficiency, eq. (10) and apply the overall heat transfer coefficient, eq. (11) to calculate ( $U_{o, cal.}$ ).

A comparison for verification should be established with the assumed value of ( $U_{o, ass.}$ ).

vi- At this stage the row exit air temperature ( $T_{ae, cal.}$ ) can be estimated which should be compared with the assumed value at stage (iii) of the solution marching of the condenser design from the following expression:

$$T_{ae, cal.} = T_i - (T_i - T_{ai}) e^{-NTU} \quad (16.a)$$

Where

$$NTU = \frac{U_{o, cal.} A_{o, ass.}}{\dot{m}_a c_{pa}} \quad \dots \quad (16.b)$$

If the assumed and calculated values of the row exit air temperature were within acceptable limit, then the calculation is terminated for this row. The exit air temperature ( $T_{ae, cal.}$ ) will be considered as the inlet air temperature to the next row as ( $T_{ai}$ ) and so on to the last row of the condenser. After the calculations have been satisfied for all condenser rows the exit of the last row temperature ( $T_{ae, cal.}$ ) will represent the calculated actual leaving temperature out of the condenser.

#### Model Verification:

The case study selected for the purpose of the model verification of the present work is that directed by the heat exchanger characteristics shown in **table (1)**. The operating conditions of the steam and air sides are listed in **table (2)**. *Abood* (2007) [22] has found that the best design criteria of the inclined condenser was at ( $30^\circ$ ) inclination from the horizontal, this conclusion will be applied at the present work for the verification of the present model.

#### Results and Discussion:

The above case study of the condenser will be used to show the

effect of the cooling of air prior to entering the condenser. The correlation for prediction of the condensation heat transfer coefficient presented by *Kutateladze* [15] will be used in the present analysis, eq.(4).

The air velocity of the air cooled heat exchangers is considered to be the vital character which determines the heat exchanger overall dimensions and establishes the face velocity. It is usually falls within the range of (1.5) to (4) m/s. *This criteria will be used as a guide for the present work simulation of the existing heat exchanger and design steam condensers.* The same original operating conditions, pressure and temperature, on the steam side were considered for all of the suggested designs.

#### Constant Air Flow Rate:

**Table (3)** is prepared for the objective of weighting the effect of entering air temperature on the performance capability of the *existing condenser* design. In this table, the air mass flow rate and the entering air wet bulb temperature were kept at a constant value corresponding to that of the original design (8102) kg/hr and ( $24^\circ\text{C}$ ) respectively. In producing these characteristic designs, the temperature of air was allowed to decrease from the original design temperature of ( $45^\circ\text{C}$ ) gradually to a minimum value of ( $26^\circ\text{C}$ ).

#### Overall Heat Transfer Coefficient:

The results showed that the mean overall heat transfer coefficient ( $U_o$ )



and heat exchanger effectiveness  $\epsilon$ ) are essentially remain at a constant value independent of the condenser load and entering air condition over the whole tested range of operation conditions of the condenser. This of course was due to the dependence of the heat exchanger performance on the air side heat transfer coefficient. The corresponding values of the mean overall heat transfer coefficient and heat exchanger effectiveness were (80 to 82)W/m<sup>2</sup>.K and (71%) respectively. The mean heat transfer coefficient on the air side showed almost a constant value regardless of the entering air temperature which in turn produces similar mean overall heat transfer coefficients of the heat exchanger for the original and the suggested designs.

However, the present model showed that there is a variation for the local overall heat transfer coefficient with row position in the air direction towards the exit side of the condenser, **figure (5)**. This is mainly due to the reduction of the air side heat transfer coefficient with row position in the air direction. The latter is a result of the thermal properties variation those controlled by the air temperature variation across the heat exchanger.

**The Condenser Steam Loading:**

**Figure (6)** represents the variation of the condenser consumption of steam mass flow rate with air side entering dry bulb temperature. It is obvious that reducing the steam condenser entering air temperature will increase the heat exchanger

capability of handling higher steam mass flow rate. The rate of increase of the steam mass flow rate with the entering air temperature reduction showed values ranged between (1.95) and (2) estimated from the following expression:

$$R_m = \frac{\dot{m}_2 - \dot{m}_1}{(T_{in})_1 - (T_{in})_2} \dots\dots\dots (17)$$

This ratio reveals that reducing the entering air temperature by (1) degree will improve the steam condensing by (2) kg/hr and increases the steam loading of the condenser. For the present case study the results showed an increase for the steam capability by (22.5 %) when the entering air temperature was reduced from the original design value of (45)°C to (26)°C.

It is obvious that the condenser steam loading varies linearly with the entering air dry bulb temperature, **figure (6)**. The data listed in **table (3)** were used to correlate the steam loading in a power form as a function of the entering air temperature to the condenser as follows:

$$\dot{m}_{cond} = C T_{in}^n \dots\dots\dots (18)$$

In which (C) and the exponent (n) are constants of the fit, their corresponding values were (759.12) and (-0.4644) respectively where ( $\dot{m}_{cond}$ ) in (kg/hr) and air dry bulb temperature ( $T_{in}$ ) in (°C).

**The Condenser Load:**

The variation of the condensation load of the heat exchanger with the entering air temperature is shown in **figure (7)**. It is clear that lowering the

dry bulb temperature of the air at the entering side of the condenser produces an increase to the condenser load depending on the reduction percent of this temperature. For the present work, an increase of (22.5%) for the condenser load for the temperature reduction of (45) °C to (26)°C shown in **table (3)**. The corresponding rate of load variation with air entering temperature change showed a range fell within (1.2) to (1.25) for the above temperature range calculated from:

$$R_Q = \frac{Q_2 - Q_1}{(T_{in})_2 - (T_{in})_1} \dots\dots\dots (19)$$

Although, the temperature difference of the suggested designs was higher than the original design, but the air exit temperature on the lee side of the heat exchanger for the suggested designs was lower than that of the original design. This in turn will achieve a quantitative higher mean temperature which acts to increase the condensation load of the heat exchanger. When the entering air temperature was reduced from (45)°C to (26)°C, the mean temperature difference was increased from (40)°C to (53.4)°C. This yield that the effective driving force of temperature to be increased by about (34 %), **table (3)**, which raised the condenser load.

The condenser load exhibited a linear variation with the entering dry bulb air temperature to the heat exchanger. Applying the data of the condenser load shown in **table (3)**, resulted in an expression for the

condenser load ( $Q$ ) as a function of ( $T_{in}$ ) in a form similar to that shown in eq.(18). In which the constant ( $C$ ) and the exponent ( $n$ ) were (471.71) and (-0.465) respectively where ( $Q$ ) in (kW) and ( $T_{in}$ ) in (°C).

**Variable Air Flow Rate:**

The existing designed heat exchanger has been investigated for different flow rate of entering air. The results of this category are shown in **table (4)** for increasing air mass flow rate up to (10502) kg/hr which corresponds to a percentage of increase around (23%). For this air mass flow rate passing through the present heat exchanger will improve its thermal load by (50%) at air entering dry bulb and wet bulb temperatures of (28)°C and (24)°C respectively. This improvement of the condenser performance corresponds to (2.5) times that of the condenser load at the same operating conditions with air mass flow rate of (8102) kg/hr. The effectiveness of the heat exchanger for these conditions exhibited a reduction to a value of (64%) for design (7) as shown in table (4). The corresponding values of condensation load and effectiveness when entering air mass flow rate was increased to (9627) kg/hr and air entered at (30) °C were (1.38) times and (66%) respectively.

This enhancement of the condensation load is mainly due to the increase of the overall heat transfer coefficient and the potential

temperature difference driving force. Beyond this air mass flow rate, the air face velocity will highly increase from the optimum recommended value of (4) m/s. Noting that the design of heat exchanger shown in **table (3)** was based on a value of (3.6) m/s.

#### Conclusions:

The present work has shown the following findings concerning the performance of air cooled condenser under dry cooling processes:

- 1- A thermal design model for the air cooled condenser has been built successfully to predict the overall dimensions of the steam condenser. This model was based on the row by row marching technique towards the exit side of the air stream from the heat exchanger.
- 2- The rate of increase of the steam mass flow rate with the entering air temperature reduction at fixed air mass flow rate showed values ranged between (1.95) and (2) kg/hr per each degree reduction of air dry bulb temperature. The corresponding values of load variation was within (1.2) to (1.25) kW/K.
- 3- Increasing the air mass flow rate by (23%) with lowering the entering air dry bulb temperature to (28)°C improved the condenser load by (2.5) times that of the original design.
- 4- Both of the condensation steam loading and the condenser load

exhibited a linear relation with the entering air dry bulb temperature. Applying the air cooling mode can greatly improve the condenser thermal load and can be used either alone or as combination with water cooling condensers in power plants.

#### References:

- [1] Larinoff, M. W. and Moles, W. E., "Design and Specification of Air Cooled Steam Condensers", Chemical Engineering, Vol. 110, pp. 143-156, (1978).
- [2] Ganapathy, V., "Applied Heat Transfer" Penn Well Publishing Company, (1982).
- [3] Micheletti, W. C. and Burns, J. M., "Comparison of Wet and Dry Cooling Systems for Combined Cycle Power Plants ".Utility Water Act Group, November (2000).
- [4] Kroeger D.G. "Air –cooled Heat Exchanger and Cooling Tower" by New York Begell House, (1998).
- [5] Berger, N., "Dry Cooling Systems for Large Power Stations", Publ. GEA Energietechnik GmbH, (1992).
- [6] Environmental Protection Agency (EPA) Rule 316 (b), New Facility Rule, Chapter 3: Energy Penalties and Chapter 4: Dry Cooling, Publ. EPA, (2000).
- [7] Maulbetsch, J. and DiFilippo, M., "Spray Enhancement of Air Cooled Condensers", Consultant Report to Electric Power Research Institute, California Energy Commission, September (2003).

- [8] Tarrad, A.H. and Shehhab, U.S., "The Prediction of Environment Effect on Performance of a Vapor Compression Refrigeration System in Air Conditioning Application", Engineering and Development Journal, Vol. 11, No.1, (2007).
- [9] Tarrad, A.H., Saleh, F.A., and Abdulrasool, A.A., "A Simplified Numerical Model for a Flat Continuous Triangle Fins Air Cooled Heat Exchanger Using a Step by Step Technique", Accepted for Publication in Journal of Engineering and Development, Baghdad, Iraq, (2009).
- [10] Nusselt, W., "Die Oberflächenkondensation des Wasserdampfes", Z. Ver. Dtsch. Ing., Vol. 60, pp. 541-569, (1916).
- [11] McAdams, W. H., "Heat Transmission", 3<sup>rd</sup> edition, McGraw-Hill Book Company, New York, (1954).
- [12] Dhir, V. K. and Lienhard, J. H., "Laminar Film Condensation on Plane and Axisymmetric Bodies in Non-uniform Gravity", J. Heat Transfer, Vol. 93, pp. 97, (1971).
- [13] Rohsenow, W. M., "Heat Transfer and Temperature Distribution in Laminar Film Condensation", Trans. ASME, Vol. 78, pp. 1645, (1956).
- [14] Kutateladze, S. S., Fundamentals of Heat Transfer, Academic Press, New York, (1963).
- [15] Kirkbride, C. G., "Heat Transfer by Condensing Vapors on Vertical Tubes", Trans. Of AIChE, Vol. 30, pp. 170, (1934).
- [16] Lubuntsov, D. A., "Heat Transfer in Film Condensation of Pure Steam on Vertical Surfaces and Horizontal Tubes", Teploenergetika, Vol. 4, pp. 72, (1957).
- [17] McQuiston, F.C., "Heating Ventilating and Air Conditioning", Analysis and Design, 3<sup>rd</sup> Edition, (1988).
- [18] Schmidt, T. E., "La Production Calorifique des Surface Munies D'ailettes", Annexe Du Bulletin De L'Institut International Du Froid, Annexe G-5, (1946).
- [19] Tarrad, A. H., Khudor, D. S., and Abdul-Wahed, M., "A Simplified Model for the Prediction of the Thermal Performance for Cross Flow Air Cooled Heat Exchangers with a New Air Side Thermal Correlation", Engineering and Development Journal, Vol. 12, No.3, Al-Mustansiriya University, Baghdad, Iraq, (2008).
- [20] Sinnott, R. K., Chemical Engineering, Vol. 6, Heaton, A. W. and Co. LTD, Exeter, (1983).
- [21] Incropera, F. P. and De Witt, D. P., "Introduction to Heat Transfer", 2nd Edition, John Wiley & Sons Inc. Publication company, (1990).
- [22] Abood, S. A., "Experimental and Theoretical Model Design of Dry Air Cooled Condenser in Power Plant", PhD. Thesis, Mechanical Engineering Department, College of Engineering, Al-Mustansiriya University, Baghdad, Iraq, (2007).

**Nomenclature:**

<b>Variable</b>	<b>Definition</b>	<b>Units</b>
$a_n$	Polynomial fit constants, $n=0,1,2$ , and 3	(---)
$A_c$	Cross sectional area	( $m^2$ )
$A_f$	Fin exposed area to heat exchange	( $m^2$ )
$A_i$	Inside tube surface area	( $m^2$ )
$A_{min}$	Minimum flow area on the air side	( $m^2$ )
$A_o$	Total outside surface area, bare tube and fins	( $m^2$ )
$cp$	Specific heat at constant pressure	(kJ/kg. K)
$D$	Diameter	(m)
$fp$	Fin pitch	(m)
$fpm$	Fins per meter of tube length	(1/m)
$g$	Gravitational acceleration	( $m/s^2$ )
$G_{max}$	Maximum mass velocity of fluid	( $kg/m^2 s$ )
$h_a$	Air enthalpy	(kJ/kg)
$h_c$	Steam condensing heat transfer coefficient	( $W/m^2 K$ )
$h_f$	Fouling factor	( $W/m^2 K$ )
$h_{fg}$	Latent heat of vaporization of water	(kJ/kg)
$h_o$	Air side heat transfer coefficient	( $W/m^2 K$ )
$H$	Heat exchanger height	(m)
$j$	Colburn j-factor defined by eq. (9)	(---)
$k$	Thermal conductivity	( $W/m. K$ )
$l$	Continuous plate fin length	(m)
$L$	Character defined by fig. (3) or tube length	(m)
$m$	Parameter defined by eq. (10) or constant in eq. (12)	(---)
$\dot{m}$	Fluid mass flow rate	(kg/s)
$M$	Character defined by fig. (3)	(m)
$n$	Number of tub rows	(---)
$N_r$	Number of tubes per row	(---)
$N_t$	Total number of tubes	(---)
$Nu$	Nusselt number	(---)
$p$	Perimeter of tube	(m)
$P$	Operating absolute pressure of steam	(bara)
$Pr$	Prandtl number	(---)
$\dot{Q}$	Condensation load	(kW)
$r$	Radius of tube	(m)
$Re$	Reynolds number	(---)
$t$	Thickness	(m)
$T$	Fluid Temperature	( $^{\circ}C$ or K)
$\Delta T_i$	Inlet temperature difference at heat exchange	(K)
$\Delta T_o$	Exit temperature difference at heat exchanger	(K)
$\Delta T_m$	Mean temperature difference of heat exchanger	(K)
$u$	Steam velocity	(m/s)
$U_o$	Overall heat transfer coefficient of condense	( $W/m^2 K$ )
$W$	Heat exchanger width	(m)

$W_a$	Specific humidity of air	(kg st/kg. d.a)
$x_t$	Short dimension of elliptical tube shape	(m)
$X_T$	Transverse tube pitch to flow direction	(m)
$X_L$	Longitudinal tube pitch in flow direction	(m)
$y_t$	Long dimension of elliptical tube shape	(m)
$Z$	Heat exchanger depth in the flow direction	(m)

**Greek Symbols:**

Variable	Definition	Units
$\beta$	Parameter defined by eq. (9.e) and eq. (9.h)	(---
$\psi$	Parameter defined by eq. (9.d)	(---
$\eta_f$	Fin efficiency defined by eq. (9.b)	(---
$\eta_{so}$	Total surface efficiency defined by eq. (9.a)	(---
$\phi$	Parameter defined by eq. (9.g)	(---
$\nu$	Kinematic viscosity	(m <sup>2</sup> /s)
$\theta$	Inclination angle from horizontal axis	(°)
$\nu$	Specific volume	(m <sup>3</sup> /kg)

**Subscripts:**

Variable	Definition
$a$	Air
$ass.$	Assumed value
$c$	Condensate
$cal.$	Calculated value
$e$	Equivalent or exit
$est.$	Estimated value
$f$	Fouling or fin
$i$	Inside or inlet
$l$	Liquid
$o$	Outside
$row$	Row value
$s$	Steam value
$Tube$	Tube value
$v$	Vapor
$w$	Wall value

**Table (1) Heat Exchanger Geometry**

	Parameter	Dimension
Core	Width ( $W$ )	700 mm
	Depth ( $Z$ )	90 mm
	Height ( $H$ )	850 mm
	No. of Tubes	276
	No. of Tube Rows	4
	No. of Tubes/Row	69
	No. of Fins/ Tube	268
	Normal Distance ( $X_T$ )	10 mm
	Longitudinal Distance ( $X_L$ )	24 mm
Fin	Pitch ( $fp$ )	3 mm
	Length ( $l_f$ )	9 cm
	Area of Single Fin ( $A_f$ )	.10265 m <sup>2</sup>
	Thickness ( $t_f$ )	0.15 mm
	Material	Copper
Tube	Width ( $W_{tube}$ )	3 mm
	Depth ( $D_{tube}$ )	19 mm
	Thickness ( $t_{tube}$ )	0.152 mm
	Material	Brass
Area	Total Surface Area ( $A_{total}$ )	35 (m <sup>2</sup> )
	Total Fin Surface Area	27.5 (m <sup>2</sup> )
	Total Bare Tube Area	7.5 (m <sup>2</sup> )

**Table (2) The Characteristics of the Case Study Design of a Typical Air Cooled (30°) Inclined Condenser.**

Characteristic Property	Original Dry Design
The Condenser Condensation Load ( kW )	80.3
Steam Operating Pressure ( bara )	1.21
Steam Operating Temperature ( K )	378.15
Steam Mass Flow Rate ( kg/hr )	129.6
Air Entering Temperature Dry/Wet (°C) / (°C)	45/24
Air Leaving Temperature Dry/Wet (°C) / (°C)	80/31.1
Air Mass Flow Rate ( kg/hr )	8102
Entering Air Face Velocity m/s	3.6
Total Surface Area (Fins & Bare) (m <sup>2</sup> )	35
Total Fin Surface Area (m <sup>2</sup> )	27.5
Total Bare Tube Area (m <sup>2</sup> )	7.5
Mean Overall Heat Transfer Coefficient (W/m <sup>2</sup> K)	82

**Table (3) A Comparison of Performance of the Dry Cooled Condenser Design at Fixed Air Mass Flow Rate.**

Case Study	$\dot{Q}_{Cond}$ (kW)	$\dot{m}_{Cond}$ (kg/hr)	$T_{in}/T_w$ (°C)/(°C)	$T_{out}/T_w$ (°C)/(°C)	$U_o$ (W/m <sup>2</sup> K)	$R_m$ (kg/hr K)	$R_Q$ kW/K
Original Design	80.3	129.6	45/24	80/31.1	82	-----	-----
Design (1)	86.5	139.6	40/24	77.7/31.5	81.5	2	1.24
Design (2)	91.4	147.5	36/24	75.8/31.9	81.2	1.98	1.23
Design (3)	96.4	155.5	32/24	74/32.3	80.8	2	1.25
Design (4)	101.2	163.3	28/24	72.1/32.7	80.6	1.95	1.20
Design (5)	103.64	167.2	26/24	71.2/32.9	80.4	1.95	1.22

**Table (4) The Performance of the Dry Cooled Condenser at Variable Air Flow.**

Case Study	$\dot{Q}_{Cond}$ (kW)	$\dot{m}_{Cond}$ (kg/hr)	$\dot{m}_{air}$ (kg/hr)	$T_{in}/T_w$ (°C) / (°C)	$T_{out}/T_w$ (°C) / (°C)	$U_o$ (W/m <sup>2</sup> K)	$\epsilon$ (%)
Original Design	80.3	129.6	8102	45/24	80/31.1	82	71
Design (6)	110.5	178.2	9627	30/24	70.5/32.1	85	66
Design (7)	120.5	194.4	10502	28/24	68.5/32.1	86	64



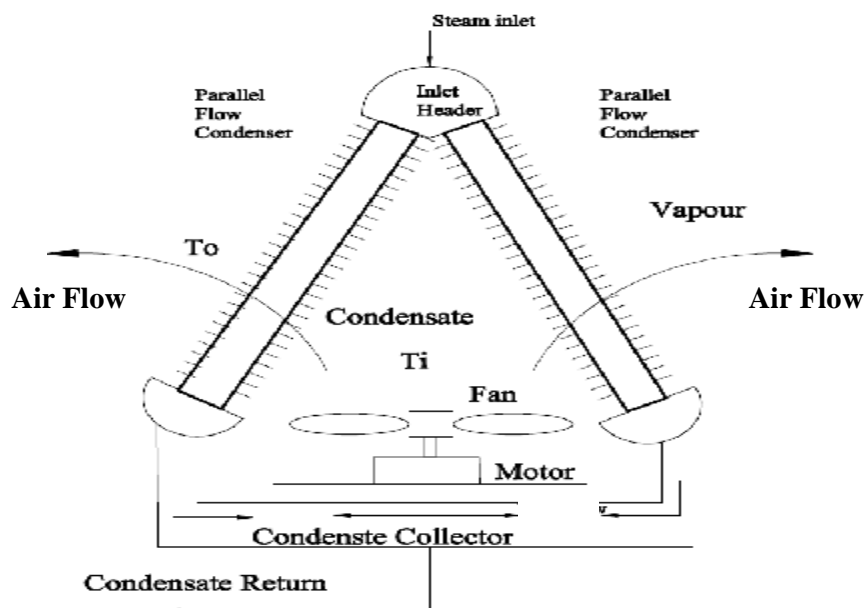


Figure (1) The Condenser Structure and Arrangement of A-Frame Type.

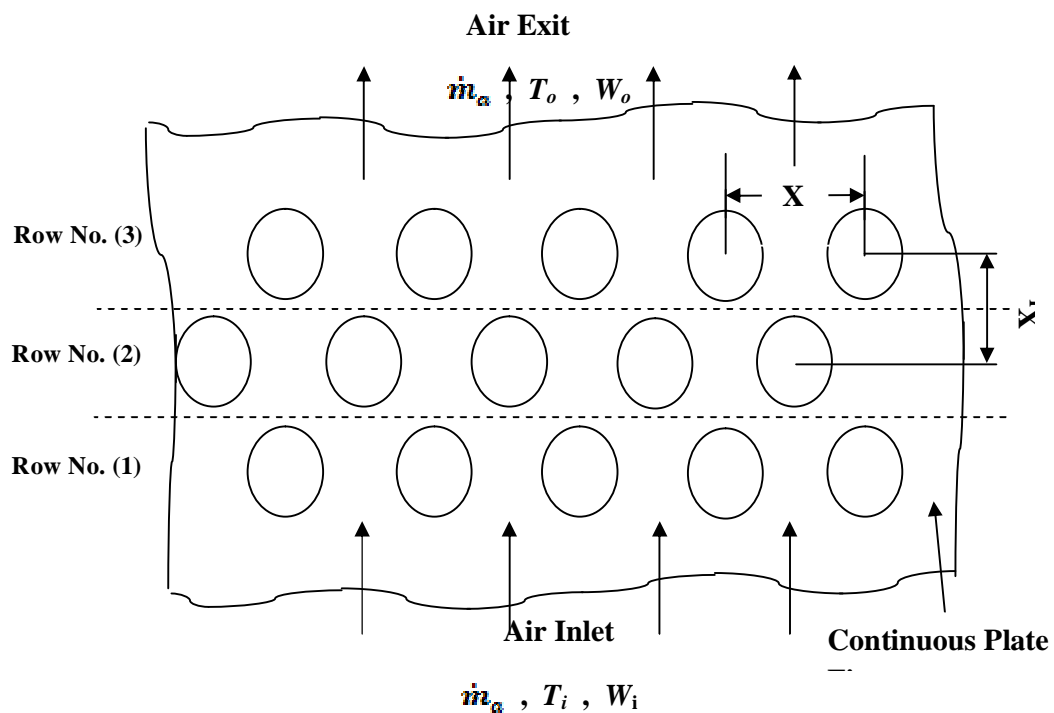


Figure (2.a): Staggered Layout

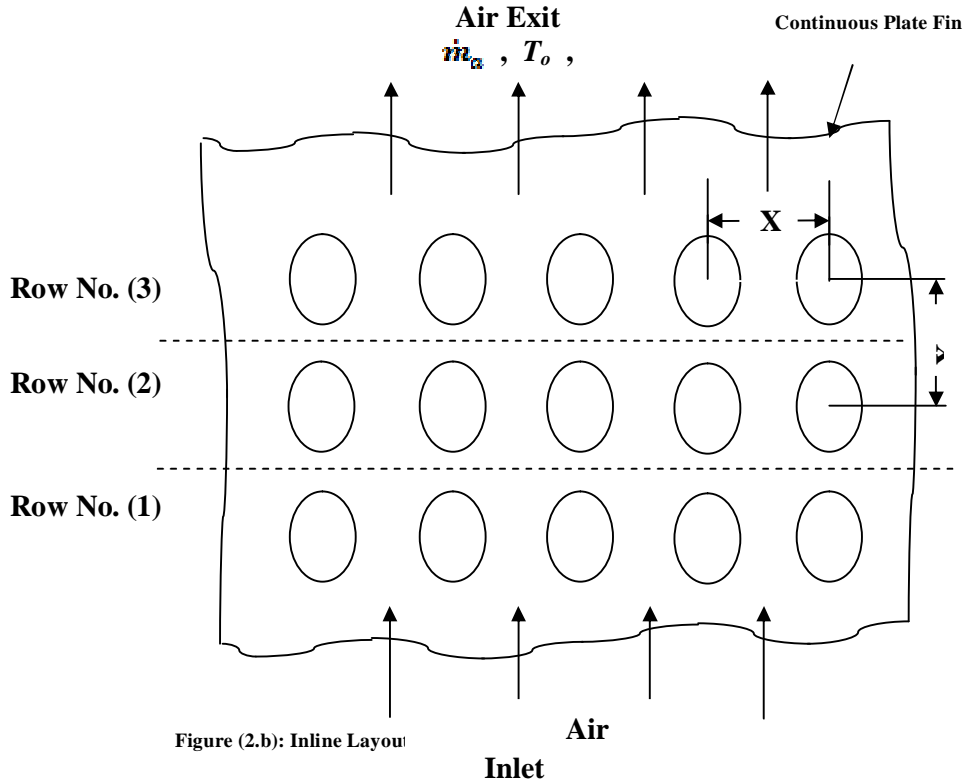


Figure (2.b): Inline Layout

Figure (2) The Tube Arrangements of Air Cooled

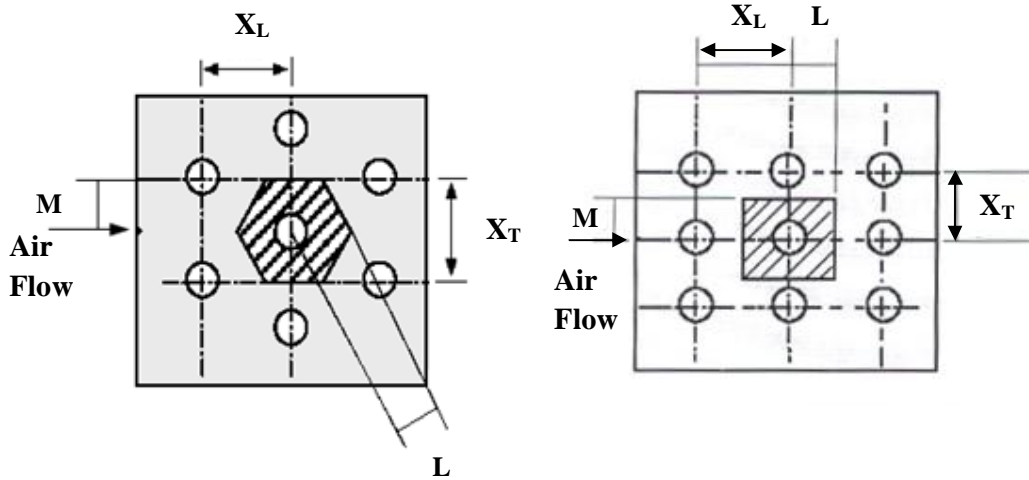


Figure (3.a) Staggered Layout

Figure (3.b): Rectangular Layout

Figure (3): The Hexagonal Continuous Plate Fin, Schmidt [18].

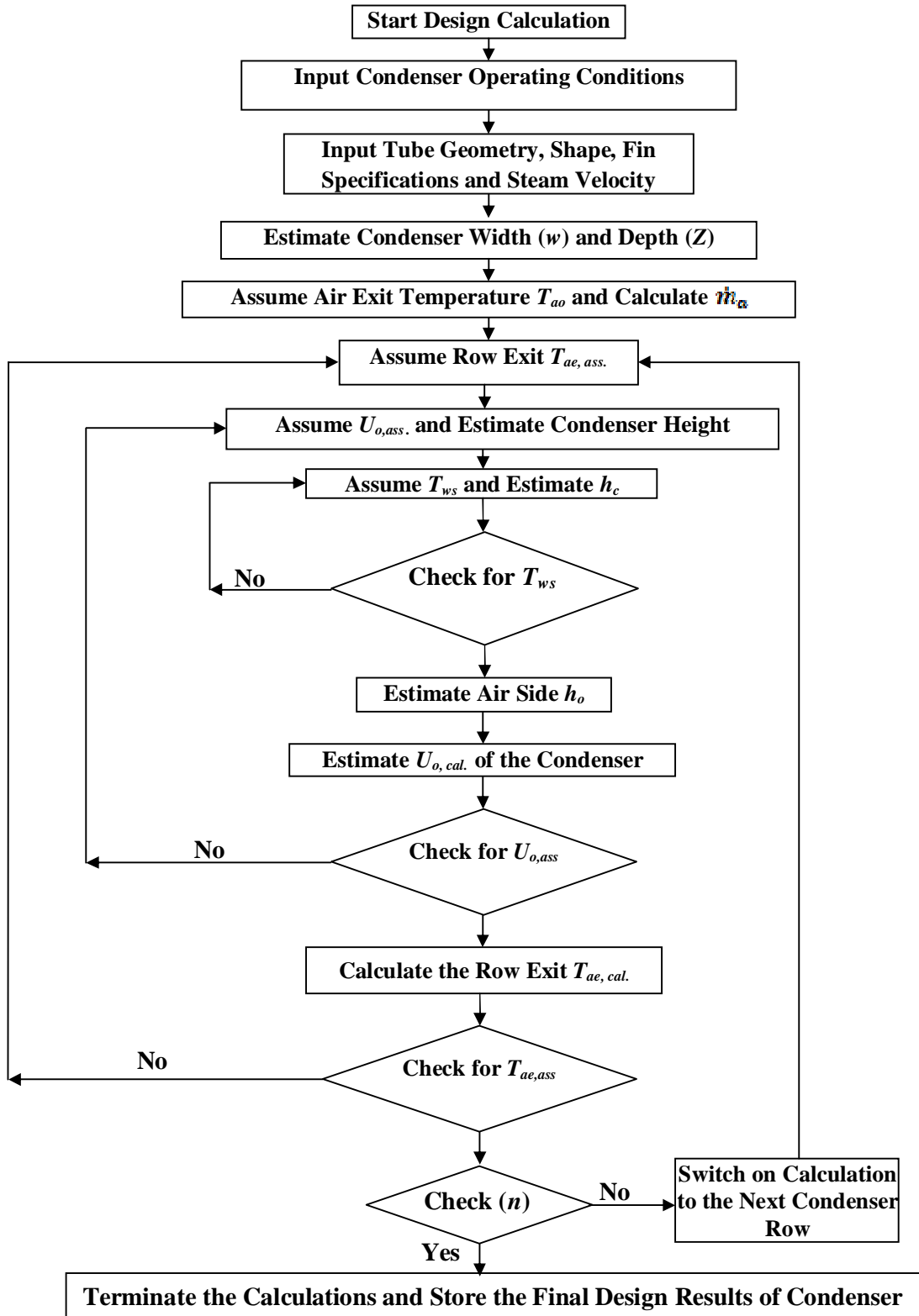


Figure (4) The Flow Chart of the Suggested Design Procedure.

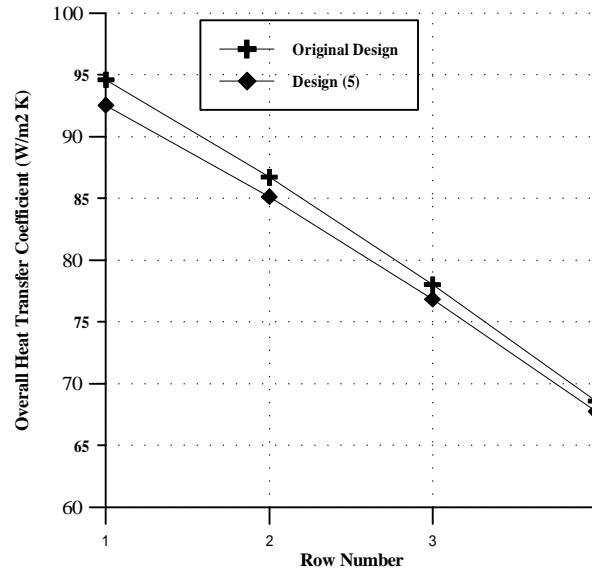


Figure (5) Overall Heat Transfer Coefficient Variation With Tube Row Position.

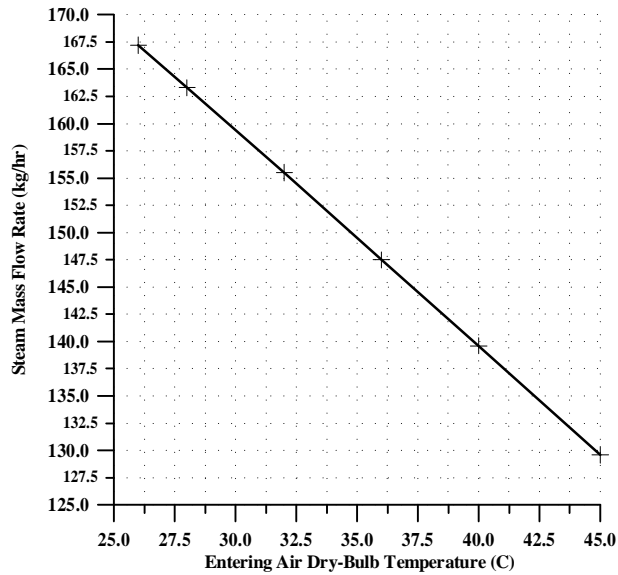
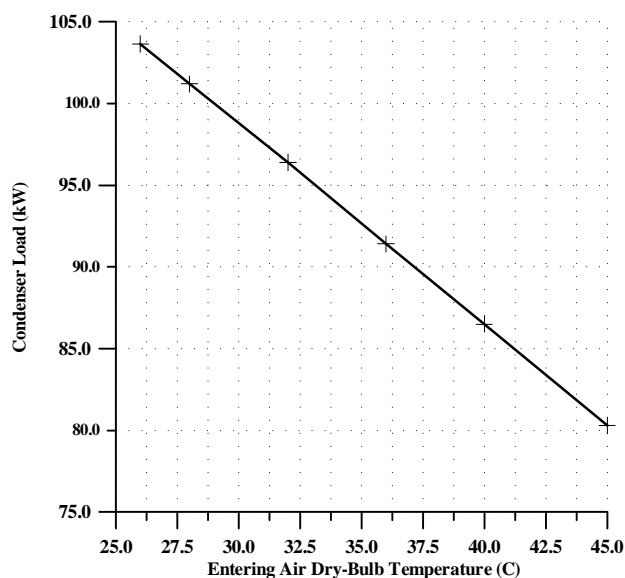


Figure (6) The Condenser Steam Loading Variation With Entering Air Dry-Bulb Temperature.



**Figure (7) The Condenser Load Enhancement With Reduction of Entering Air Dry-Bulb Temperature.**